IL NUOVO CIMENTO **46 C** (2023) 126
DOI 10.1393/ncc/i2023-23126-6

COMMUNICATIONS: SIF Congress 2022

Iron oxide nanoparticles as agents for combined therapy and magnetic resonance imaging

F. BRERO(1), P. CALZOLARI(2), M. ALBINO(3), A. ANTOCCIA(4), P. AROSIO(2), M. AVOLIO(5), F. BERARDINELLI(4), D. BETTEGA(2), M. CIOCCA(6), A. FACOETTI(6), S. GALLO(2)(*), F. GROPPI(2), C. INNOCENTI(3), A. LAURENZANA(7), C. LENARDI(2), S. LOCARNO(2), S. MANENTI(2), R. MARCHESINI(2), M. MARIANI(5), F. ORSINI(2), E. PIGNOLI(8), C. SANGREGORIO(3), F. SCAVONE(7), I. VERONESE(2) and A. LASCIALFARI(5)(1)

(1) *INFN, Sezione di Pavia - Pavia, Italy*
(2) *Dipartimento di Fisica and INFN, Università degli Studi di Milano - Milano, Italy*
(3) *ICCOM-CNR and Dipartimento di Chimica, Università di Firenze - Sesto Fiorentino, Italy*
(4) *Dipartimento di Scienze and INFN, Università Roma Tre - Roma, Italy*
(5) *Dipartimento di Fisica, Università degli Studi di Pavia - Pavia, Italy*
(6) *Fondazione CNAO - Pavia, Italy*
(7) *Dipartimento di Scienze Biomediche Sperimentali e Cliniche "Mario Serio" - Firenze, Italy*
(8) *Fondazione IRCSS Istituto Nazionale dei tumori - Milano, Italy*

received 23 February 2023

Summary. — Multifunctional iron-oxide based nanoparticles for magnetic fluid hyperthermia (MFH-therapy) and magnetic resonance imaging (MRI-diagnostics) have been investigated for their morpho-dimensional characteristics and relaxometric properties. The nanoparticles were constituted of a spherical Fe_3O_4 core with diameter $d = 19.2 \pm 3.6$ nm, coated with meso-2,3-dimercaptosuccinic acid (DMSA). The ^{1}H NMR results showed a longitudinal r_1 relaxivity curve typical of high-anisotropy materials and a transverse relaxivity that, at clinical field $\mu_0 H = 1.5$ tesla, was $\sim$3 times higher than the one of commercial MRI contrast agents. The system displayed a SAR $\sim 110 \pm 30$ W/$g_{Fe_3O_4}$, *i.e.*, high enough to allow for a successful combination of MFH-assisted-hyperthermia and hadron therapy on pancreatic tumor cells.

1. – Introduction

Most diffused applications of magnetic nanoparticles (MNPs) in the biomedical field concern the imaging field [1], the drug and gene delivery [2], the cell tracking, the magnetic fluid hyperthermia (MFH) [3], and other therapy and diagnostic techniques, either combined or not [4,5]. Thanks to their biocompatibility, versatility, good magnetic properties (superparamagnetism) and low cost, nanoparticles based on iron oxides (IONPs)

(*) Corresponding author. E-mail: salvatore.gallo@unimi.it

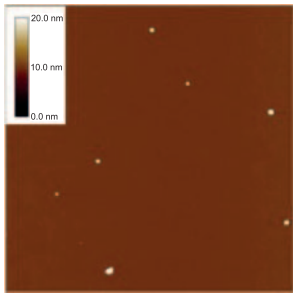

Fig. 1. – AFM topography image of the investigated sample. Single IONPs and small IONPs aggregates are visible on the mica support; the image was collected in air, in tapping mode. Scan area: $2 \times 2\,\mu\text{m}^2$. Vertical color scale range: 0–20 nm.

are the most used [6]. IONPs, generally dispersed in a water-based solution, are constituted of a core of iron oxide small crystals, which is coated with an organic shell to guarantee biocompatibility, optimize colloidal stability, protect iron leaching, and provide specific sites to graft chemical moieties with specific biological functions (*e.g.*, drug delivery and release) [7]. It is worth reminding that IONPs are extensively studied as magnetic resonance imaging (MRI) T_2-CAs (Contrast Agents) because they efficiently shorten the transverse relaxation time (T_2), thus decreasing the MRI signal on T_2-weighted images and enhancing contrast. On the other hand, in MFH they are used to release heat locally under an applied alternating magnetic field (AMF), thus leading *e.g.*, to tumor cells death through apoptosis with minimum side effects [8]. Within this general framework, we explored the use of IONPs as MRI-CAs and as heating mediators for MFH combined with hadron therapy (HT). The ^{1}H NMR transverse relaxivity resulted much higher than the one of the previously commercial CA Endorem®, thus envisaging a possible clinical use with reduced doses. On the other hand, the relatively high specific absorption rate (SAR) allowed performing successfully combined HT+hyperthermia treatments [9,10] on pancreatic tumor cells cultures.

2. – Materials and methods

AFM imaging. – Atomic force microscopy (AFM) imaging was performed using a Nanoscope Multimode IIId system operating in air in tapping-mode.

NMR measurements. – The NMR-dispersion profiles were collected at room temperature by measuring the longitudinal T_1 and the transverse T_2 relaxation times ($10\,\text{kHz} < \nu < 60\,\text{MHz}$). Details on sequences are reported in [11].

Hyperthemia combined with Hadron Therapy. – Carbon ion and proton irradiations were performed at Centro Nazionale di Adroterapia Oncologica (Pavia, Italy). Photon beam irradiation was performed at Fondazione IRCCS Istituto Nazionale dei Tumori (Milano, Italy). Hyperthermia was obtained by means of a thermalization system surrounding the samples, assisted by Magnetic Fluid hyperthermia. See [9, 10] for more details.

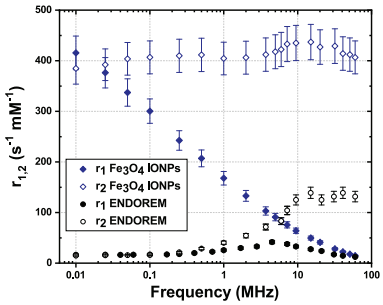

Fig. 2. – Longitudinal (r_1) and transverse (r_2) relaxivity ^{1}H-NMR profile of Fe_3O_4 IONPs, collected at room temperature. The Endorem values are shown in gray.

3. – Experimental results and discussion

Morphological, structural, magnetic and hyperthermic properties of used IONPs samples are reported in [9] and [10]. Briefly, the investigated sample consists of a core made of spherical Fe_3O_4 IONPs with diameter $d = 19.2 \pm 3.6$ nm, coated by DMSA. Magnetometry results indicated that MNPs display a superparamagnetic behavior, as expected for magnetite-based particles of this size. From AFM imaging (fig. 1), the IONPs overall (magnetic core plus DMSA shell coating) diameter resulted $d_{\mathrm{AFM}} = 20.3 \pm 2.7$ nm. This result indicates a shell thickness of about 1 nm, accordingly to other results reported in literature for this particles size and coating [12]. As concerns the ^{1}H NMR measurements (fig. 2), it is worth reminding that the nuclear longitudinal ($i = 1$) and transversal ($i = 2$) nuclear relaxivity r_i is defined as $r_i = \frac{1}{c} \cdot (\frac{1}{T_{i,m}} - \frac{1}{T_{i,dia}})$ where c is the concentration of the paramagnetic centers, $1/T_m$ the measured relaxation rates, and $1/T_{dia}$ the relaxation rates in the presence of the dispersant only. We observed the following trends. First, the sample shows a continuous increase of the longitudinal nuclear relaxivity r_1 by lowering the Larmor frequency with no detectable maximum, and at high frequency (>10 MHz) it exhibits the common behavior led by the Ayant spectral density (which reflects the Langevin function and the τ_D-guided spin dynamics). The low frequency behavior can be explained qualitatively by taking into account the contribution to the Freed spectral density function, due to a high energy barrier related to the crystal's internal (high) magnetic anisotropy; the theory [13] predicts a r_1 flattening for low frequency for spherical ferrite-based particles with core diameters above approximately 15 nm. It is worth

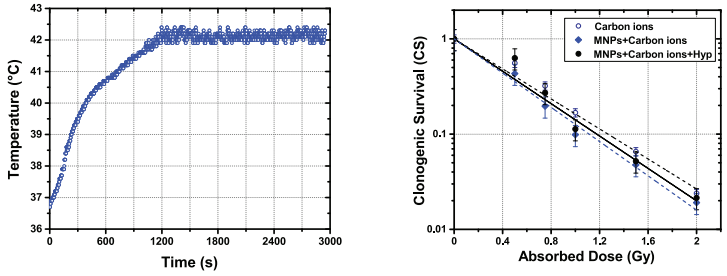

(a) (b)

Fig. 3. – (a) Heat release experiments on BxPC3 cells cultures (T $\sim$42°C for 30 min, see [9, 10] for more details). (b) Clonogenic survival of BxPC3 cells culture for 3 different protocols: carbon ion irradiation only, irradiation + MNPs administration and irradiation + MNPs administration + hyperthermia treatment.

noting that here, instead of a clear flattening of $r_1(\nu)$, an increase is present with a slight tendency to flatten below 0.02 MHz. Secondly, the NMR-dispersion profiles of the previously (no longer used since 2012) commercial CA Endorem display lower values of longitudinal and transverse relaxivity over the whole frequency range, thus suggesting that our IONPs are more efficient CAs. In particular, at relatively high magnetic field $\mu_0 H \sim$1.41 tesla (close to the clinical one), r_2 reaches the value $\sim 407\,\mathrm{mM^{-1}s^{-1}}$, approximately three times the r_2 value of Endorem. As concerns Hyperthermia on cells, the SAR value of our MNPs in water dispersion in an applied AMF of frequency 109.8 kHz and amplitude 19.5 mtesla, resulted to be $\sim 110 \pm 30\,\mathrm{W/g_{Fe_3O_4}}$. In fig. 3(a) we show the temperature increment of BxPC3 cells cultures during the hyperthermia treatment, and in fig. 3(b) the renormalized clonogenic survival of BxPC3 cells subjected to carbon ion irradiation only, irradiation and MNPs, irradiation plus MNPs and MFH-assisted Hyperthermia. From fig. 3(b) and from the results published in [9] and [10], it can be easily deduced that for all the three types of irradiation (photons, carbon ions and protons) investigated, the MNPs plus hyperthermia treatment grants a further killing effect, compared to the single irradiation, that results to be synergistic in case of proton irradiation, and additive for carbon ion irradiation (for more details, see refs. [9] and [10]).

4. – Conclusions

We presented experimental results of AFM characterization, NMR relaxometry, SAR, and clonogenic survival, on ferrite-based MNPs with about 19 nm core diameter, and a DMSA coating. The investigated MNPs are good candidates for being theranostic systems, carrying out a dual-function: i) improving the MRI contrast, due to a transverse relaxivity which is 3 times the one of previously marketed Endorem; ii) releasing heat for MFH therapy, as they show relatively high SAR $\sim 110 \pm 30\,\mathrm{W/g_{Fe_3O_4}}$ values [9, 10]. Concerning the future steps of this work, two main lines can be traced: a) when performing MFH for cancer treatment, the surrounding healthy tissue often suffers from collateral heat damage, due to a non-precise IONPs localization inside the tumor; to avoid this, a specific image guidance is needed and IONPs could be helpful MRI contrast agents for this purpose, although problems due to susceptibility artifacts should be overcome; b) the possible combined action of HT and MFH on 3D cellular scaffolds loaded with tumor cells, thus mimicking the *in vivo* situation, will be carefully investigated within a vision of future translation to the clinic.

REFERENCES

[1] Han X. *et al.*, *Nanoscale*, **11** (2019) 799.
[2] Kami D. *et al.*, *Int. J. Mol. Sci.*, **12** (2011) 3705.
[3] Etemadi H. and Plieger P. G., *Adv. Ther.*, **3** (2020) 2000061.
[4] Farzin A. *et al.*, *Adv. Healthcare Mater.*, **9** (2020) 1901058.
[5] Brero F. and Gallo S., *Int. J. Mol. Sci.*, **23** (2022) 13770.
[6] Gambhir R. P. *et al.*, *Appl. Surf. Sci. Adv.*, **11** (2022) 100303.
[7] Socoliuc V. *et al.*, *Magnetochemistry*, **6** (2020) 2.
[8] Das P. *et al.*, *Colloids Surf. B: Biointerfaces*, **174** (2019) 42.
[9] Brero F. *et al.*, *Nanomaterials*, **10** (2020) 1919.
[10] Brero F. *et al.*, *Nanomaterials*, **13** (2023) 791.
[11] Brero F. *et al.*, *Nanomaterials*, **10** (2020) 1660.
[12] Avolio M. *et al.*, *J. Magn. Magn. Mater.*, **471** (2019) 504.
[13] Roch A. *et al.*, *J. Chem. Phys.*, **110** (1999) 5403.